ACADEMIA
MATERIALS SCIENCE

Research Article
Published: 2025-07-02
https://doi.org/10.20935/AcadMatSci7795

Flowability of NbC-based cermets for additive manufacturing via L-PBF

Rodrigo Condotta[1,*], Fabio Miranda[2,3], Nathalia M. G. Pereira[1], Marcelo O. dos Santos[1,4], Daniel Rodrigues[3], Suzilene R. Janasi[3], Fernando S. Ortega[3,5], Gilmar F. Batalha[6]

Academic Editors: Raul D.S.G. Campilho

Abstract

Niobium-based refractory alloys have attracted attention in several industrial areas, such as metalworking, steelmaking, military, and armoring applications, among others. The production of these refractory alloys using additive manufacturing techniques, specifically selective laser fusion in a powder bed (L-PBF), has been a major challenge; this is primarily due to the complex optimization of the sintering process parameters required to obtain dense parts, free of porosity or cracks, and to achieve highly homogeneous layers in the powder bed. However, the success of L-PBF is highly dependent on the physical properties of the powders used in the process. Key factors such as good flowability, reduced particle size and narrow distribution, sphericity, and density influence powder spreading, powder layer uniformity, and the final part integrity. Furthermore, properties of the composite, such as hardness, toughness, and wear resistance, can be modified by changing the cermet composition, which could also negatively impact its flowability. This work aims to evaluate the physical properties of NbC-based cermets with different compositions to better understand their influence on metallic powder flowability. Optimizing powder properties and flowability through processing parameters is crucial for L-PBF to fully harness the potential of NbC-based cermets, thereby paving the way for their broader adoption in high-performance applications.

Keywords: *metal powders for L-PBF, NbC-based cermets, powder flowability, granules' rheological properties*

Citation: Condotta R, Miranda F, Pereira NMG, dos Santos MO, Rodrigues D, Janasi SR, et al. Flowability of NbC-based cermets for additive manufacturing via L-PBF. *Academia Materials Science* 2025;2. https://doi.org/10.20935/AcadMatSci7795

1. Introduction

Cermets, a class of composite materials combining ceramic and metallic phases, have gained significant attention due to their unique balance between hardness, wear resistance, and toughness [1]. These materials are widely used in applications requiring extreme mechanical and thermal stability, such as cutting tools, wear-resistant coatings, and aerospace components [2]. The chemical composition and physical characteristics of cermets strongly influence their properties, particularly particle size distribution and flowability, which play crucial roles in their processing and final performance [3].

The chemical composition of cermets determines their fundamental properties, such as hardness, toughness, oxidation resistance, and thermal stability [1, 3]. Transition metal carbides, such as titanium carbide (TiC), tungsten carbide (WC), and niobium carbide (NbC), are commonly used as ceramic reinforcements, while metals like cobalt (Co) and nickel (Ni) act as the binder phase. The choice of binder influences the material's toughness and processability, making it a critical factor in cermet design [4].

During the development of additive manufacturing (AM) technology, numerous terms and definitions have been used in different technical fields, such as selective laser sintering (SLS) and selective laser melting (SLM). Often, concerning specific application areas and registered trademarks, the terms SLS and SLM are examples of this, generating ambiguity and confusion among engineering professionals, technicians, and researchers. Laser Powder Bed Fusion (L-PBF) is the general nomenclature used to define the digital additive manufacturing process. It has been used more frequently by several industrial sectors to reduce the production costs of components with complex geometries, mainly for the manufacture of high-value, low-volume mechanical components and for complex shapes.

The two techniques are identical; what differentiates SLM from SLS is that SLM is more common for obtaining dense metals, requires more energy and rapid cooling, and can generate more residual stresses and distortions. On the other hand, SLS is more commonly used for polymers, requires less thermal energy from the laser, and does not completely melt the powder [5]. Unlike conventional casting or subtractive manufacturing techniques, L-PBF enables precise control over microstructure and mechanical properties [6–8]. However, the materials must exhibit specific

[1]Department of Chemical Engineering, Centro Universitário FEI, São Bernardo do Campo 09850-901, Brazil.
[2]Instituto de Pesquisas Energéticas e Nucleares, São Paulo 05508-000, Brazil.
[3]BRATS Sintered Filters and Special Powder Composites, Cajamar 07750-620, Brazil.
[4]Department of Mechanical Engineering, Instituto Mauá de Tecnologia, São Caetano do Sul 09580-900, Brazil.
[5]Institute of Research and Development, Universidade do Vale do Paraíba, São José dos Campos 12244-000, Brazil.
[6]Department of Mechatronics and Mechanical Systems Engineering, Polytechnic School of USP, University of São Paulo, São Paulo 05508-010, Brazil.
*email: rcondotta@fei.edu.br

physical properties for successful implementation, including optimal powder flowability, controlled particle size distribution, low agglomeration tendency, and high thermal stability.

L-PBF's ability to produce near-net-shape components with minimal material waste and its capacity to manufacture intricate geometries that are difficult or impossible to achieve using traditional methods make it a highly attractive option for the aerospace, biomedical, and high-performance tooling industries [9, 10].

In addition to composition, the physical properties of cermet powders significantly affect their behavior during processing, especially in additive manufacturing (AM) techniques like L-PBF. Particle size distribution impacts packing density, layer uniformity, and final part density, whiles flowability governs the ease of powder deposition and spreading across the powder bed. Poor flowability can result in irregular layers, leading to defects such as lack of fusion, increased porosity, and residual stresses. Hence, one of the main challenges in L-PBF is achieving uniform powder deposition across the powder bed, which directly influences the mechanical integrity of the final part [10, 11].

For the direct sintering technique, the behavior of the metal powder is a critical parameter. The powder flow for deposition is a complex phenomenon that needs to be understood or even modeled. The properties of metal powders are sensitive to external factors such as relative humidity (%), geometric sizes and shapes, or voltages applied between the particles. Other factors that also contribute to the deposition flow are the surface roughness and oxidation state, the apparent density, and the electrostatic and magnetic characteristics of the material. This complexity significantly affects the powder bed's flowability, whether in terms of flow or cohesiveness. If the powders are more cohesive than expected, this can limit the deposition flow, reduce powder bed homogeneity, and negatively impact the quality of the final product. Therefore, accurately characterizing the powder feed flow behavior for a specific process is extremely important [11, 12].

Spherical metal powders manufactured for the L-PBF process are considered ideal powders for the production of sintered parts, as they have uniform sizes, smooth surfaces, and fine sizes with good flowability, and are capable of providing a continuous flow in the nozzles or feeding ducts. In addition, they have low porosity and high density. However, these are high-cost metal powders [10, 11]. In contrast, conventional metallurgy powders typically have high surface roughness due to their coarse surface textures and irregular shapes.

Thus, flowability is one of the key properties of cermet powder to be evaluated for maintaining consistency in layer deposition and ensuring high-density parts with minimal defects. Flowability is mainly influenced by particle morphology, size distribution, surface roughness, and the presence of agglomerates. Particle sizes to be used in L-PBF are typically in the range of 10 to 60 μm, and it is well-known that the flowability of particles below 100 μm is problematic due to their cohesive behavior [12]. However, surface modifications and flow agents can enhance powder behavior, reducing the risk of segregation and improving spreadability [13].

The application of NbC-based cermets in AM has gained traction as industries seek to optimize their performance for high-precision and complex geometries. The L-PBF process, in particular, presents challenges due to the inherent difficulties in processing ceramic–metal composites. Issues such as poor powder flowability, heterogeneous microstructure formation, and cracking due to thermal stresses require careful optimization of process parameters and powder characteristics [7].

In our previous studies [14, 15], the production of NbC-based alloys using different processes was investigated, as many industries—such as aerospace, biomedical, and tooling—are exploring the potential of NbC-based cermets in additive manufacturing (AM) for producing components with superior wear resistance and lightweight properties. However, those studies only discussed the final parts' microstructures, porosities, and hardness.

The scope of this study is to evaluate how the properties of NbC-based cermets, including composition, particle size, and mainly flowability indicators, influence their properties and processability in AM, addressing key challenges and proposing strategies for process optimization.

2. Materials and methods

2.1. NbC cermet preparation

Pure commercial Co, Ni, NbC, and WC were used to prepare samples of powdered composites of NbC-based alloys. Small amounts of WC were added to NbC-based powder mixtures due to its ability to inhibit grain growth and promote the formation of fine-grained carbides during the sintering process [16, 17]. Additionally, it reinforces the metal matrix by increasing the dissolution of WC in the metallic binder phase (Co and Ni), which enhances the hardness of the binder up to a certain level and contributes significantly to improvements in both overall hardness and fracture toughness (K_{IC}) [18]. Although no sintering process was carried out in this study, the presence of a typical 3.0 wt.% WC in the powder mixture may still influence its flowability.

Table 1 presents the properties of all the commercial metallic powders, as evaluated in a previous study, including particle and bulk densities, purity, and particle size, while **Figure 1** shows the particle morphology.

Table 1 • Properties of ceramic and metallic powders (Miranda et al. [4]).

Powder	Density (g.cm^{-3})		Particle size (μm)	Purity (%)	Origin/suppliers
	Real	Bulk			
NbC	7.65	2.82	<1.0	99.65	F&X Electro-Materials Ltd. (Jiangmen, China)
WC	15.63	4.02	1.5	99.53	Buffalo Tungsten Inc. (Depew, NY, USA)
Co	8.90	1.81	2.0	99.97	Nanjing Hanrui Cobalt Co. (Nanjing, China)
Ni	8.91	2.66	4.8	99.85	CVMR Corporation (North York, ON, Canada)

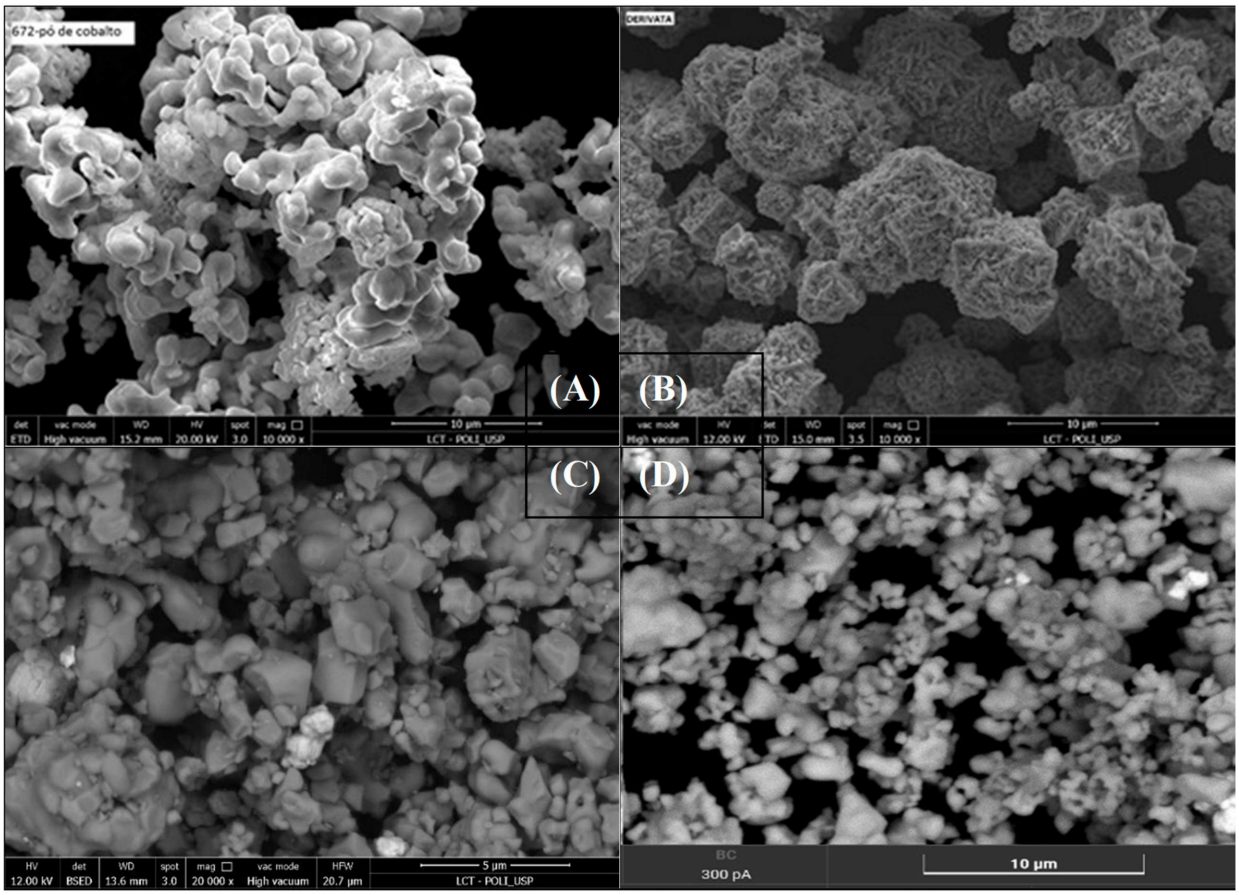

Figure 1 • SEM images of (**A**) cobalt, (**B**) nickel, (**C**) NbC raw material before being mixed in suspension, and (**D**) NbC-Co composite.

The raw materials NbC, WC, Ni, and Co were characterized according to their particle size distribution (**Figure 2**) using a laser diffraction S3550 analyzer (Microtrac, Montgomeryville, PA, USA). Analysis showed that NbC and CO powders exhibited the narrowest distributions and the smallest particles (<0.1 µm). In contrast, Co, Ni, and WC powders all displayed larger particles and broader distributions compared to NbC.

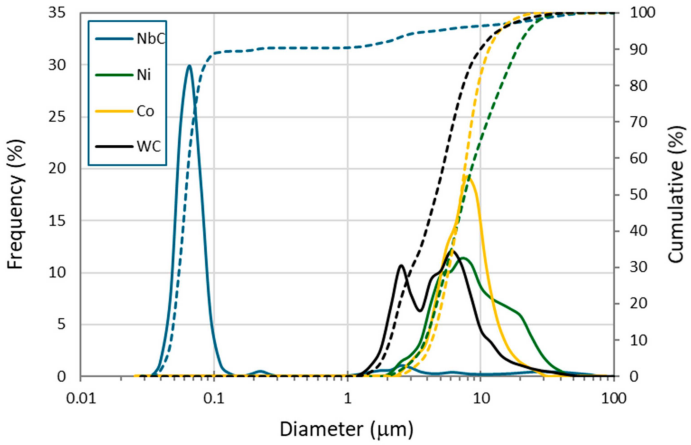

Figure 2 • Granulometric distribution of raw materials (NbC, Co, Ni, and WC) [4]: frequency distribution (solid lines) and cumulative distribution curve (dashed lines).

The true density was determined by a helium pycnometer, model AccuPyc II 1350 (Micromeritics, Norcross, GA, USA).

The composition of the prepared mixtures is detailed in **Table 2**, which shows that 3 wt.% WC was added to all mixtures. This is crucial for controlling abnormal grain growth of NbC during liquid phase sintering and improving the mechanical properties after direct sintering [18]. It is worth noting that direct laser sintering (L-PBF) is not within the scope of this analysis.

Table 2 • Weight balance and selected properties of prepared NbC alloys.

Sample	Composition (% weight)				d_{SAUTER}	Bulk density
	NbC	WC	Co	Ni	(µm)	(g.cm^{-3})
NbC-Co	67.0	3.0	30.0	0.0	139	2.01
NbC-Ni	67.0	3.0	0.0	30.0	138	1.84
NbC-Co-Ni	67.0	3.0	15.0	15.0	155	1.82

The NbC, Co, Ni, and Co/Ni combination powders were mixed using conventional powder metallurgy techniques. A MSM-B mechanical stirrer (Werner Mathis, Zürich, Switzerland) (**Figure 3A**) with a marine propeller operated at 3000 rpm for 2 h, using a 1:1 powder-to-isopropyl alcohol suspension (**Figure 3B**). Next, the isopropyl alcohol was removed by conventional drying in an oven at 200 °C for 4 h.

Figures 4–6 show SEM images (BSE/SE modes) along with their respective chemical spectra and elemental quantification. These images display the elements present in the NbC-based powder mixtures (as detailed in **Table 2**), distinguishing dark particles (Ni, Co, and NbC) from light particles (WC).

A comparative analysis of the NbC-Co (**Figure 4**), NbC-Ni (**Figure 5**), and NbC-Co-Ni (**Figure 6**) alloys reveals that WC appears as light particles. At the same time, NbC, Co, and Ni primarily differ in particle morphology. This analysis was performed using a Vega 5 LMS Scanning Electron Microscope (SEM) (Tescan, Brno, Czech Republic).

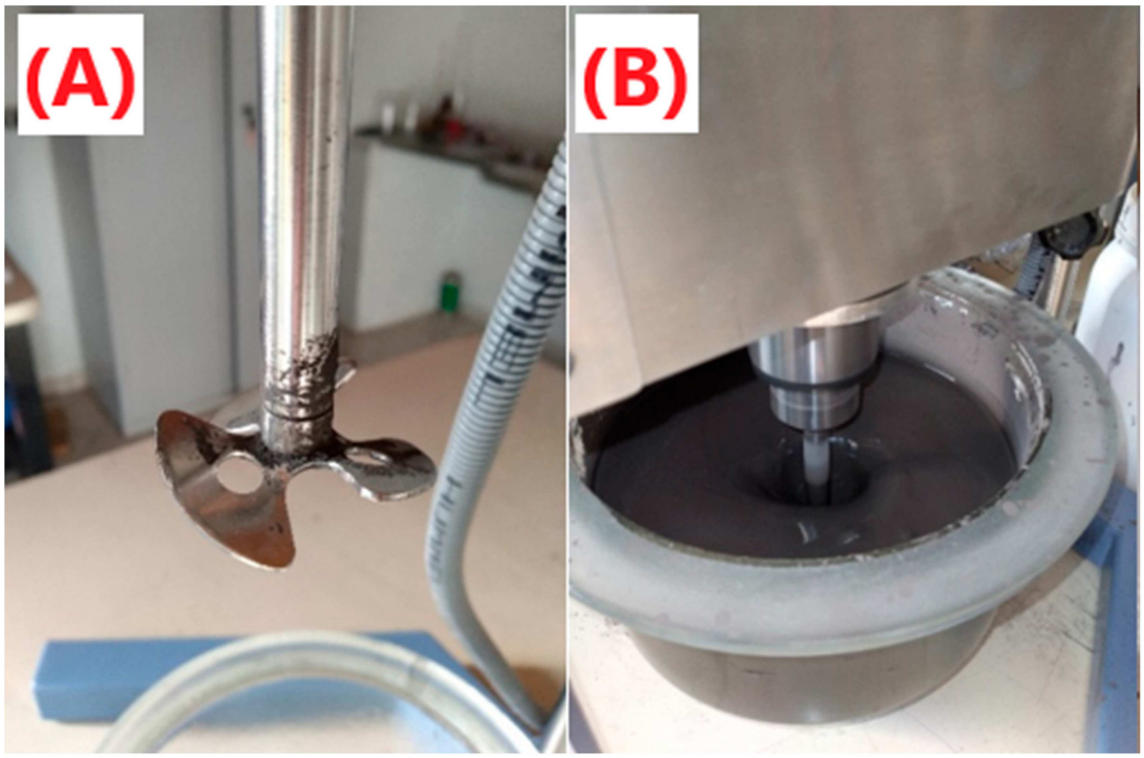

Figure 3 • Conventional mechanical agitator: (**A**) propeller in a marine-type propeller; (**B**) glass container with a maximum capacity of 5 kg for metal powder mixtures [4].

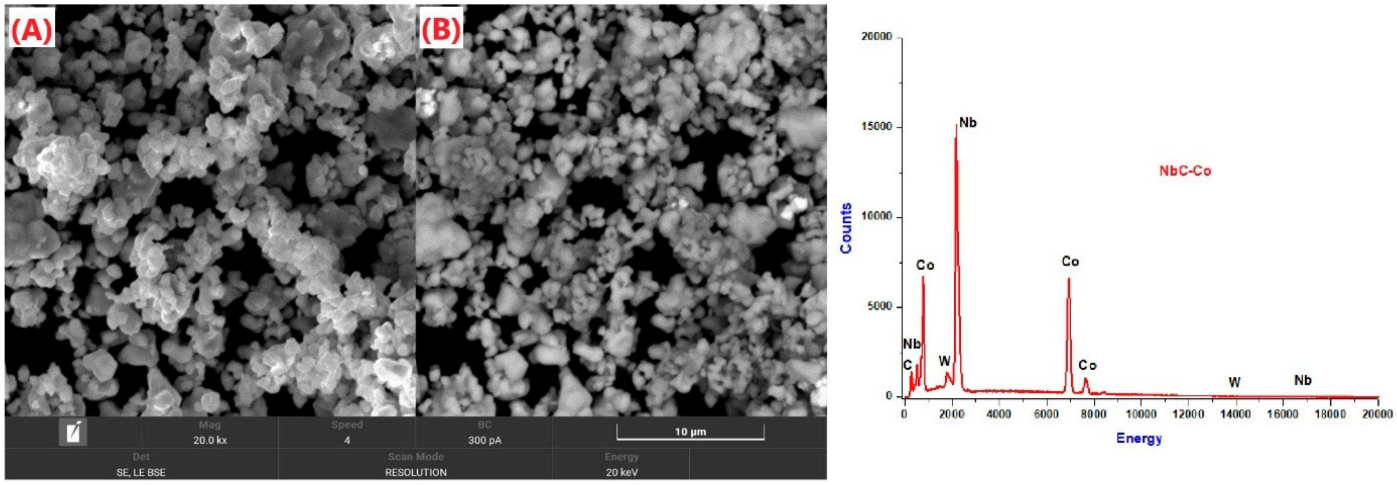

Figure 4 • SEM images (**A**) SE and (**B**) BSE of the same NbC-Co alloy and chemical spectrum–quantification of the elements in the NbC-Co powder mixture.

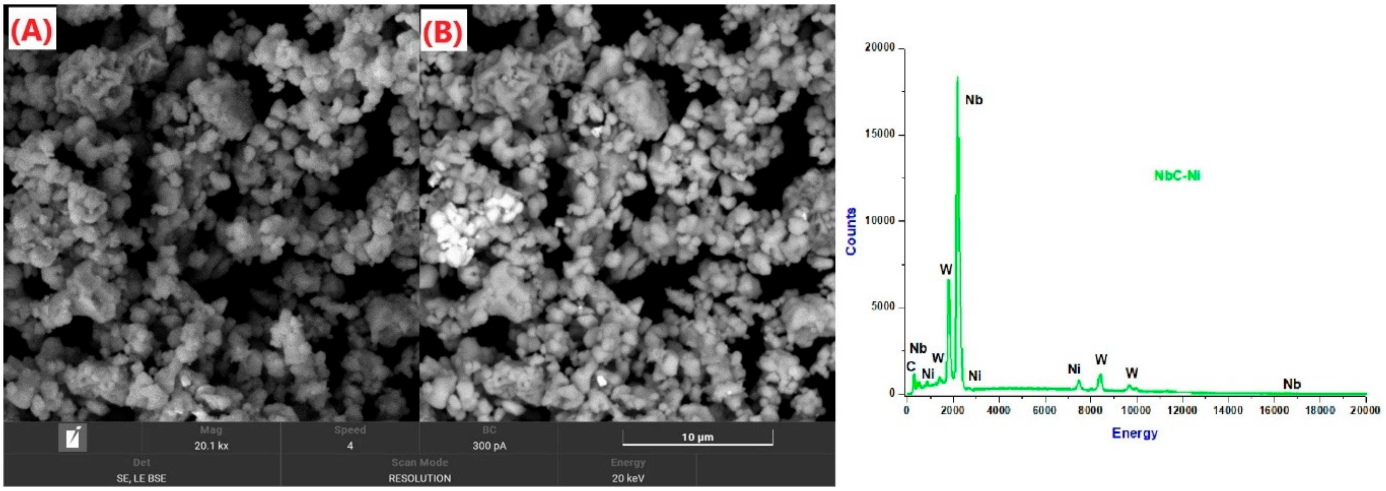

Figure 5 • SEM images (**A**) SE and (**B**) BSE of the same NbC-Ni alloy and chemical spectrum–quantification of the elements in the NbC-Ni powder mixture.

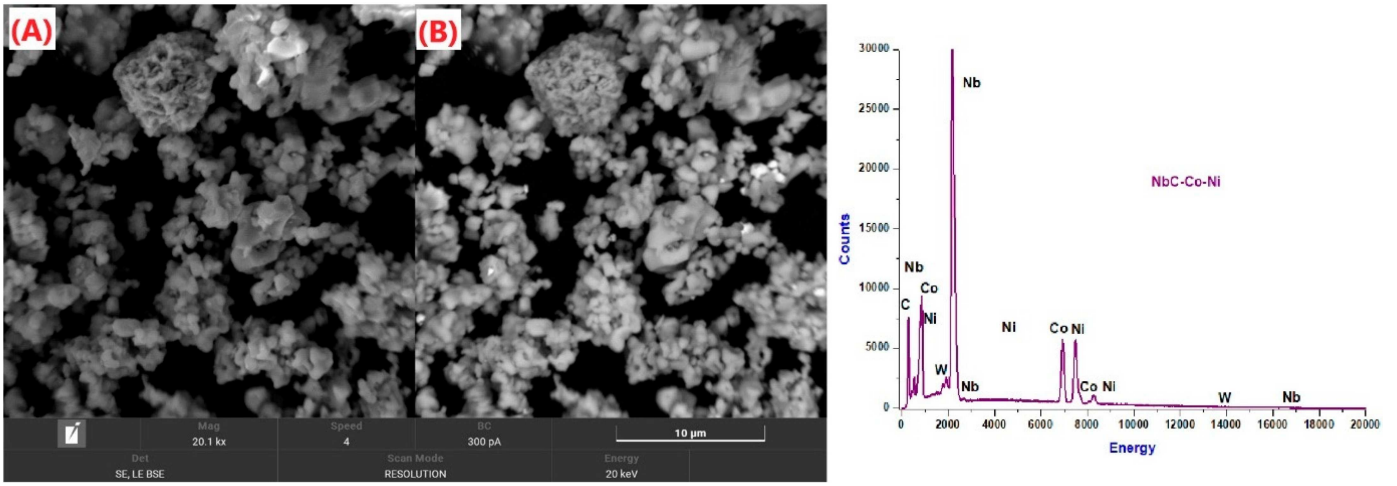

Figure 6 • SEM images (**A**) SE and (**B**) BSE of the same NbC-Co-Ni alloy and chemical spectrum–quantification of the elements present in the NbC-Co-Ni powder mixture.

A sieve shaker LGI-VW-SSO model) (LGI Scientific, São Paulo, Brazil) and a precision analytical balance were used to analyze the particle size distribution of the NbC-based mixtures. A set of standardized sieves (maximum capacity of 6 sieves) was selected. These sieves are commonly used for hard metal mixtures in manufacturing processes and feature the finest mesh sizes: # 150 mesh (100 µm), # 200 mesh (75 µm), # 325 mesh (44 µm), # 400 mesh (37 µm), # 500 mesh (25 µm), and # 600 mesh (15 µm).

2.2. Powder rheology and flowability

A FT-4 powder rheometer (Freeman Technology, Tewkesbury, UK) [19, 20] equipped with a 50 mm diameter accessory assembly was used to evaluate the dynamic properties of the powders. This involved measuring the energy expended when the powder was "bulldozed" by a twisted blade. A detailed description of this equipment and its tests can be found elsewhere in the literature, as well as the definition of some specific test parameters, such as flow rate index (FRI) and aeration ratio (AR) [13, 19, 20]. All tests were performed at least in duplicate.

The dynamic test, comprising the basic flow energy (BFE) and variable flow rate (VFR), involves a blade moving up and down along a helical path through a powder bed. Powder deformation and flow are induced by the blade's motion, with the axial and rotational components of the applied force determining the energy expenditure associated with powder redistribution. For this test, seven consecutive BFE measurements were performed at a constant blade tip speed of 100 mm/s to evaluate powder bed stability and test consistency. Subsequently, four additional tests were conducted at decreasing blade speeds (100, 70, 40, and 10 mm/s) to assess the VFR.

The compression test evaluated how bulk density varies with applied normal stress. Measurements were taken at eight consolidation states ranging from 0.5 to 15.0 kPa.

The aeration test is a BFE test conducted with air injected at the base of the powder bed. It assesses the reduction in BFE as a function of the air velocity permeating the powder bed, which fluidizes the particles and reduces interparticle contacts. **Figure 7** displays the FT-4 Powder Rheometer and the accessories used to carry out the above-described measurements.

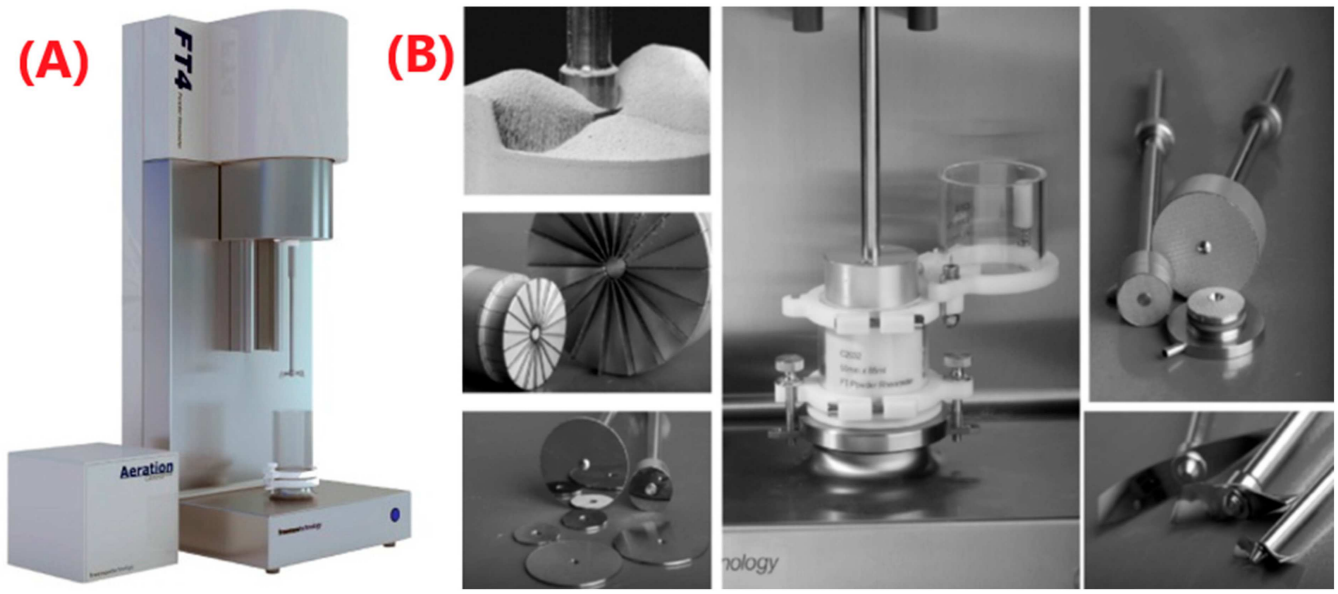

Figure 7 • FT-4 Powder Rheometer® (**A**) and its corresponding accessories and vessels (**B**) [19].

The shear experiment relies on the rheological and frictional characteristics of bulk solids and determines the cohesion of powders in a consolidated (compressed) state. To achieve these parameters, a yield locus composed of five shear points—ranging from 20% to 80% of the applied consolidation stress (3, 6, 9, and 15 kPa)—is obtained. Finally, beyond the cohesion obtained directly from the yield locus, the powder flow function (FF), which defines powder flowability, was also estimated from the major principal stress (MPS) and unconfined yield strength (UYS) [13, 20, 21].

The particles' powder characteristics and rheological properties directly influence the compacted layer in the powder bed. These properties correlate with variations in powder bed filling, compressive strength, permeability, and dynamic flow, and are predictably influenced by AM processing parameters. Further investigation into the behavior of fine and submicron powders in the dynamic regime is necessary, especially for NbC-based alloys containing particles smaller than 1 μm. This requires greater measurement repetition to better differentiate between powders with similar rheological properties across all packing states [4, 10, 11, 20].

3. Results and discussion

The evaluation of particle size distribution in powdered composites is essential across all processes aimed at the production of sintered parts. This is because particle size is intrinsically linked to the final part's density and linear or volumetric shrinkage. Coarse particles, resulting from the mixing of raw materials, underwent a sieving granulometric classification according to the Tyler system, ranging from #50 to #400 mesh (37 to 297 μm). The Sauter diameter (d_{SAUTER}) was used as the mean particle size reference. **Figure 8** shows the particle size distribution obtained using a sieve vibrator for 15 min, which was a reasonable time to allow for separation and preliminary classification of the different grain sizes of the powder samples.

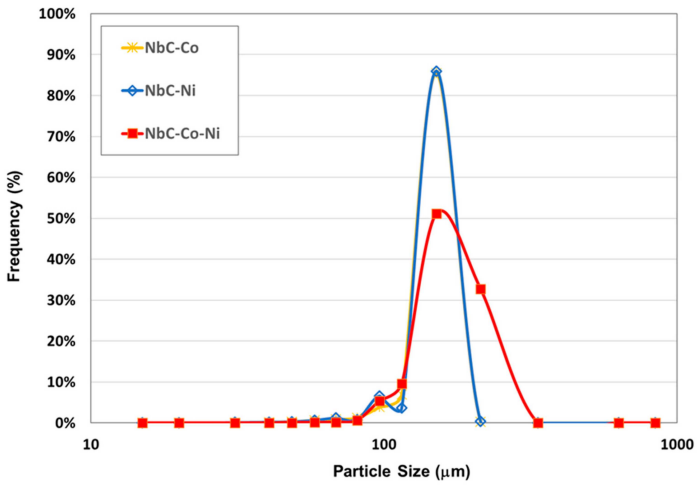

Figure 8 • Particle size distribution of pure components and NbC-based alloys.

It is observed that the particle size distributions of all three NbC-based alloy samples are monodisperse and very similar, with mean sizes ranging from approximately 138 to 155 μm. This indicates that particle size is a characteristic of the mixture process used, which causes granulation of the original smaller raw material particles. Hence, the mixing process is very consistent and reproducible.

Figure 9 shows the raw materials' basic flow energy (BFE). Ni particles exhibited the highest resistance to flow. This behavior is likely due to their irregular and coarse morphology, which causes interlocking as the blade passes through the sample. On the other hand, Co particles, being more spherical, showed the smallest and most concise BFE values. Finally, NbC presented an intermediate behavior.

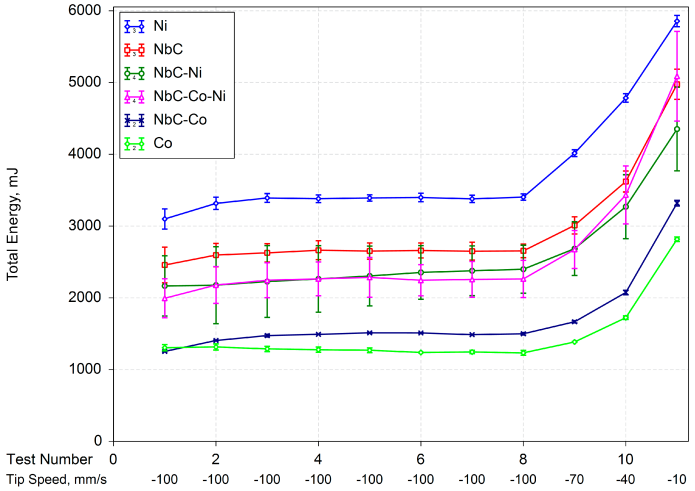

Figure 9 • Result of basic flow energy (BFE) and variable flow rate (VRF) tests.

Regarding the composites, all of them exhibited smaller BFE values compared to pure NbC samples. NbC-Co presented the smallest value, similar to pure Co metal, suggesting that Co could be an effective flowability agent for NbC. However, a similar flow pattern was observed for NbC-Ni and NbC-Co-Ni, despite the presence of Ni in the latter. This indicates that only 15% of Co is insufficient to improve NbC's flowability in these specific composite mixtures.

Another interesting behavior across all tested samples is that their BFE increases with the reduction in the blade speed. This means that the force to move the powder by an accessory doubles when the powder movement reduces to one-tenth of the initial speed. This finding is essential for developing accessories and devices that promote powder flow at very small velocities.

The compressibility of the powder composites, measured as the reduction in volume during compression (**Figure 10**), provides essential information regarding the causes of major defects or microstructural aspects. Consequently, it will influence the part's properties and application. All three composites exhibited similar compressibility, indicating they would form a powder bed with comparable compaction properties. This suggests that the nature and amount of binders in the evaluated composites will not affect the compressibility conditions; therefore, they should be selected based on another suitable property.

Better than nothing, the compressibility was also unrelated to each powder's particle size. Still, regarding their shape, rounded particles exhibited higher compressibility, while more cubic-shaped particles provided the lowest compressibility behavior.

It can also be observed that the NbC-Ni-based sample showed the highest compressed bulk density. This is particularly interesting since the loose sample was in a nonconsolidated state, suggesting that the small NbC particles effectively fill the interstitial spaces of larger Ni particles.

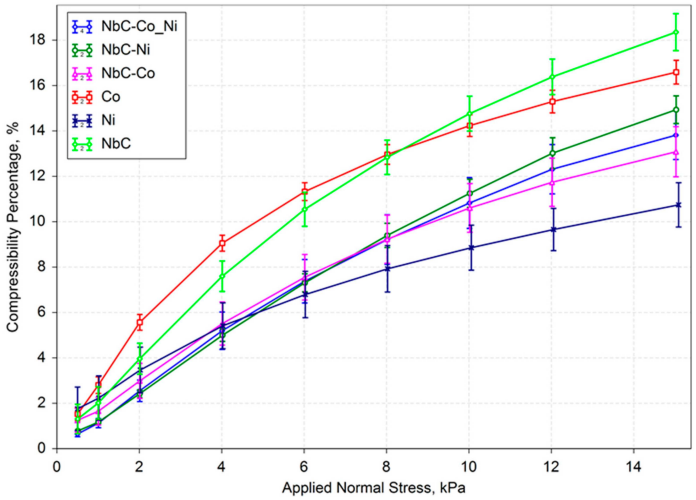

Figure 10 • Graphical results of the compressibility test of powder composites and raw materials.

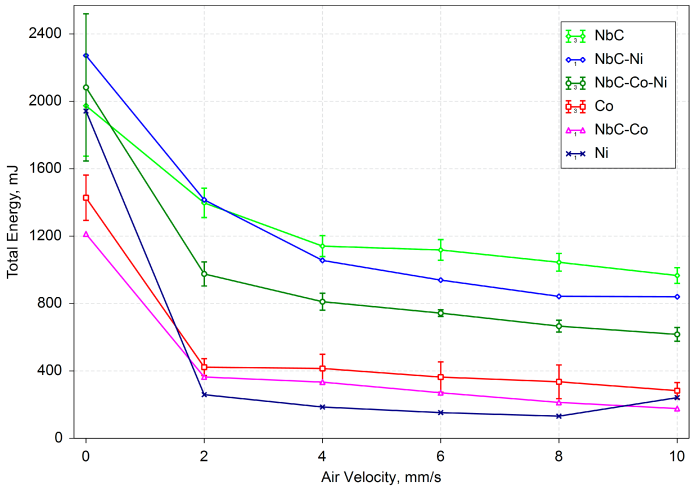

Figure 11 • Graphical results of the powder composite and raw material aeration test.

Table 3 presents the results of the BFE test and the compressibility test (subject to 15 kPa of normal stress), which also evaluated the bulk density of the samples.

Table 3 • Relationship between apparent density and compression percentage of samples.

Samples	Bulk density ($g.cm^{-3}$)	BFE (mJ)	Compressibility @ 15 kPa (%)	$BD_{comp.}$ ($g.cm^{-3}$)
NbC	2.66	2652.3	18.35	2.82
Ni	2.34	3391.4	10.74	3.00
Co	2.18	1239.4	16.59	2.18
NbC-Ni	2.26	2388.0	14.93	2.92
NbC-Co-Ni	2.40	2260.2	13.81	2.62
NbC-Co	2.45	1493.2	13.08	2.82

The aeration test serves as an indicator of the powder permeability under lower-stress conditions. While this information is not particularly useful during powder bed layer constitution in an AM process, it becomes crucial when filling die cavities or deep molds, where air must permeate the powder bed without carrying it away.

Furthermore, the aeration test indicates powder cohesion at no consolidation stress. Incipient fluidization describes the state where the particles' weight is counterbalanced by the drag force from an upward fluid flow. Generally, surface forces are more significant for small particles due to their high specific surface area. For particles with fewer interactions, airflow can easily separate them [22, 23]. If each particle is completely separated from the adjacent ones, their interactions become negligible, and the measured BFE tends to be minimal, as the blade encounters no net resistance. Conversely, a cohesive residual interaction between particles is observed as higher BFE values at the incipient fluidization condition, which is identified by a plateau in the aeration test graph (**Figure 11**).

The aeration test indicates that all powders are easily portable, as the aeration plateau is observed at a very small air velocity. When comparing the raw materials, both Co and Ni exhibited easier aeration behavior than NbC. This is likely due to the smaller particles in the NbC sample, which develop a more cohesive behavior, forming larger and denser agglomerate clusters than Co particles. This results in a higher residual BFE value even after the incipient fluidization stage.

It is also noticeable that NbC and NbC-Ni samples are more cohesive than NbC-Co. However, all binders and their mixtures enhance the powder composite's fluidization and reduce the residual BFE value under incipient fluidization conditions. Observing the results obtained in **Table 3** it is clear that powder mixtures comprising Ni require higher energy (BFE) to be moved by the blade. This behavior is similar to what was seen in the aeration test (**Figure 11**), where higher BFE values at steady state were observed for these samples. Therefore, it can be stated that the transfer of both NbC-Ni and NbC-Co-Ni powder mixtures from the container to the powder bed will exhibit low fluidity.

Cohesion may only be quantitatively estimated through a shear experiment. Results of shear experiments have proven that NbC-Ni is the most cohesive powder composite, as shown in **Figures 12** and **13**, and in **Table 4**.

Shear test results confirmed that NbC-Co is the least cohesive powder composite, corroborating the aeration test's results. This, coupled with its lower BFE, makes it the optimal composite composition for the LPB-F process, despite similar compressibility to other composites. This superior flowability is likely due to the identical particle sizes of its components (1 and 2 μm) and the nearly spherical shape of the Co particles.

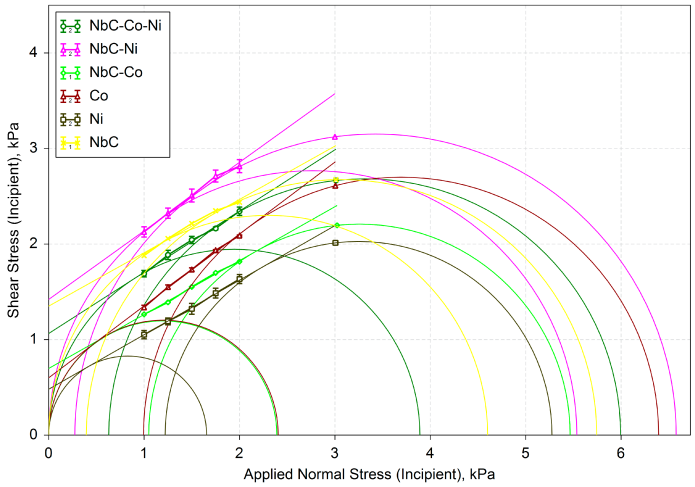

Figure 12 • Construction of the typical yield of NbC-based mixtures at 3 kPa.

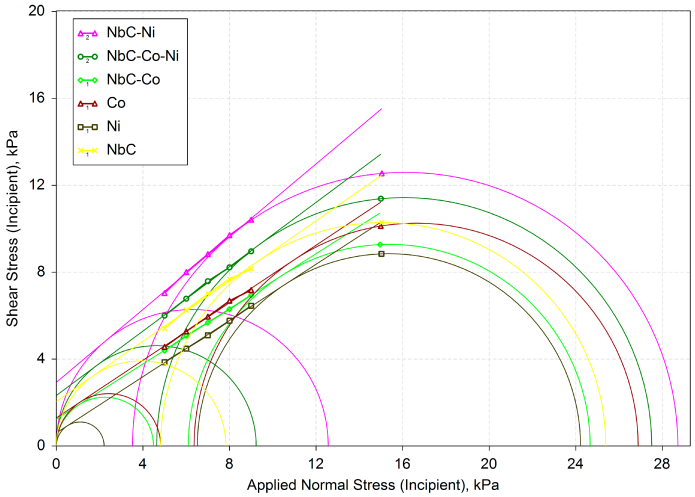

Figure 13 • Construction of the typical yield of NbC-based mixtures at 15 kPa.

Table 4 • Quantitative parameters evaluated by the shear test.

Samples	Parameter	3 kPa	6 kPa	9 kPa	15 kPa
NbC	Cohesion (kPa)	1.35	1.97	2.05	2.45
	AIF (°)	29.2	29.6	29.13	34.7
Ni	Cohesion (kPa)	0.48	0.51	0.71	0.80
	AIF (°)	29.7	31.8	31.0	32.9
Co	Cohesion (kPa)	0.60	0.87	1.11	1.29
	AIF (°)	37.0	33.8	33.7	33.5
NbC-Ni	Cohesion (kPa)	1.42	1.99	3.08	2.93
	AIF (°)	35.7	38.7	37.1	39.9
NbC-Co-Ni	Cohesion (kPa)	1.06	1.56	2.07	2.32
	AIF (°)	32.7	33.7	33.4	36.5
NbC-Co	Cohesion (kPa)	0.70	0.93	1.19	1.23
	AIF (°)	29.4	31.7	31.1	32.4

On the other hand, the composite comprising NbC and Ni particles exhibited the highest cohesion and more challenging fluidization conditions. The discrepancy in the particle sizes between the raw material and the cubic shape of Ni could contribute to this behavior.

Finally, a beneficial effect of Co was observed in the NbC-Ni sample, reducing its cohesion and enhancing its fluidization pattern, though no effect was noted on its BFE. Therefore, the inclusion of Ni in the composition of NbC-based alloys warrants careful consideration, as it leads to a significant reduction in composite powder flowability.

The Mohr circles, estimated through the experimental yield locus for each sample at the four different consolidation states, allowed for plotting the flow function of the raw materials and composites, as shown in **Figure 14**.

According to the flow function, all powders tend to become more cohesive at low stress, which is the prevailing condition during the deposition of a powder layer in the L-PBF process. For others, the powder is subject only to its weight. Moreover, the classification of all powder composites' flowability and the excellent flowability of NbC-Co composite become evident.

Miranda et al. [4] developed a pneumatic industrial turbine container (GT series with silencer connector) coupled with a metal roller. This roller's rotation speed is controlled independently of the displacement speed. In this direct sintering process, metal powder compaction is applied inside the sintering chamber. The metal powder flows under the fluidizing container and, through its translation and rotation movement, can simultaneously spread and compress. Within this device, the powder composites must flow under the fluidizing container while simultaneously being spread and compacted. The compaction of thin layers with a compacting roller is particularly interesting for extra-fine metal powders in applications focused on three-dimensional printing (e.g., SLS, SLM, 3DP, or L-PBF) [23]. Therefore, understanding the powder's behavior under these conditions (aerated, non-consolidated, and compacted) is essential for the correct setup of the device and, consequently, the properties of the final part.

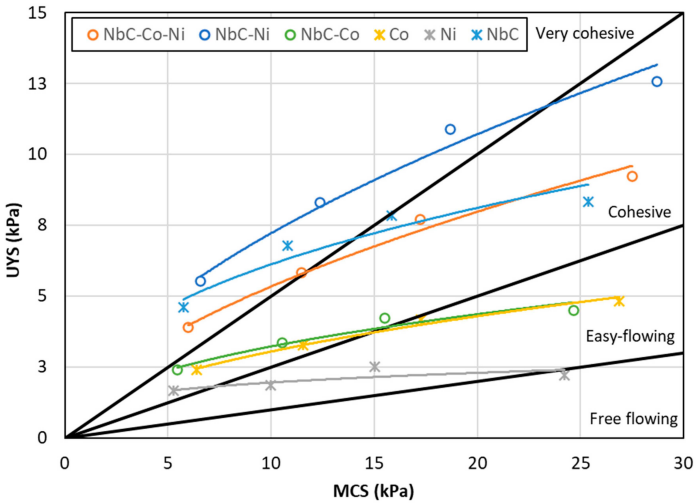

Figure 14 • Flow function of the samples estimated by the shear test.

The FT4 Powder Rheometer has emerged as a new powder flow testing device [9, 20]. Flow resistance is characterized by flow energy, defined as the sum of the rotational and translational work required to drive a rotating impeller a certain distance in a powder bed. This device can differentiate the flowability of powders that otherwise exhibit similar behavior in shear tests, partly attributable to the dynamic nature of the test. In other cases, flow energy has correlated well with other flowability measurement techniques. Currently, the device is primarily used for comparative testing rather than process design [24–26].

The differences in flowability between Co- and Ni-based NbC powders are expected to significantly impact powder bed uniformity and, consequently, the integrity of final parts produced via L-PBF. The superior flowability of NbC-Co powders, attributed to the spherical morphology and lower cohesion of Co particles, promotes a more uniform and consistent powder layer during deposition. This reduces the likelihood of defects such as uneven layer thickness, voids, or poor interlayer fusion, which can compromise mechanical properties. In contrast, the higher cohesion and reduced flowability of NbC-Ni powders, likely due to Ni's more irregular particle shape and stronger interparticle interactions, can lead to uneven spreading, increased powder bed roughness, and localized agglomeration. These effects may result in insufficient fusion, increased porosity, and residual stresses in the printed part, negatively affecting its mechanical strength and reliability. Therefore, optimizing powder flowability, particularly through binder selection, is crucial for enhancing L-PBF process efficiency and ensuring high-performance NbC-based cermet components.

The L-PBF technique is a promising alternative for NbC-based alloys with Ni and Co metal powders, which are selectively deposited and melted by a computer-controlled laser, layer by layer [24, 27]. One of the advantages of the L-PBF technique is the ability to manufacture tungsten mechanical components with complex shapes (external and internal) and small dimensions, something that cannot be easily manufactured by traditional techniques such as casting, forging, machining, and conventional powder metallurgy [9, 10, 26, 28–30]. However, not all materials suit this AM process, involving the dry powder bed deposition technique and rapid localized melting and solidification. The dry powder deposition technique is essential for AM via L-PBF. Therefore, information indicating which formulation properties make it suitable or unsuitable for this processing method is necessary, and the tests carried out via FT-4 contribute greatly, as demonstrated in this study.

4. Conclusions

This work investigated the rheology of NbC-Ni, NbC-Co, and NbC-Co-Ni powder composites, comparing them with pure Co and Ni metallic powder via FT-4 analysis. The goal was to establish critical functions, both analytically and experimentally, to advance the construction of deposited and compacted layers in the powder bed.

Here are the key findings:

I. Pure Ni binder, despite its good flowability and aeration pattern, worsened the properties of pure NbC in the NbC-Ni composite.

II. The best powder flow conditions were observed in samples containing only Co, specifically NbC-Co, exhibiting flowability comparable to WC-Co. Conversely, the NbC-Ni samples showed very poor flow.

III. The benefit of Co was also evident when added to the NbC-Ni composite, improving the flowability of this powder composite.

IV. The porosity of all evaluated NbC-based composites was similar, suggesting that a single compaction technique (device) during powder bed formation will suffice to produce a flawless part.

V. The packing of the NbC-Ni mixture indicated higher levels of cohesion than the NbC-Co- and NbC-Co-Ni-based alloys, attributable to the apparent densities of the mixtures.

VI. The mixed particles (Co, Ni, and NbC) achieved the best packing/compressibility. Larger and denser particles, such as Ni, tend to flow more freely in the powder bed, enabling them to slide over each other to form a more compacted and cohesive powder bed.

These conclusions are interesting and complementary to our previous discussion (Miranda et al. [4]), encouraging new research in this field:

A. The alloys containing the Co binder phase showed higher hardness when compared to those containing Ni and Co-Ni binders.

B. The NbC-based alloys with Ni exhibited the lowest levels of thermal residual stress, below 50 MPa (compressive stress).

Finally, to assess the impact on the additive manufacturing (AM) process, a spreadability test using these fully characterized powders should be conducted to evaluate powder bed formation.

Acknowledgments

The authors would like to acknowledge the BRATS and Centro Universitário FEI for structural support.

Funding

The authors thank the financial support provided by the São Paulo Research Foundation (FAPESP), Brazil, under grant number 2022/06201-7, linked to grant 2019/08927-2. The authors also thank the National Council for Scientific and Technological Development (CNPq) for the technological development and innovative extension scholarships, grant numbers 350485/2025-9 and 350440/2025-5, linked to the executing institution under grant 441780/2024-5.

Author contributions

R.C.: writing—original draft and editing, software, visualization, validation, and methodology, F.M.: writing—review and editing, resources, conceptualization, data curation, formal analysis, investigation, and methodology, M.O.d.S.: writing—review, formal analysis, visualization, validation, and methodology, N.M.G.P.: validation and methodology, D.R.: conceptualization, funding acquisition, project administration, resources, validation, and supervision, S.R.J.: funding acquisition, resources, validation, supervision, and conceptualization, F.S.O.: conceptualization, validation, methodology, and writing—review and editing, G.F.B.: conceptualization, validation, and supervision. All authors have read and agreed to the published version of the manuscript.

Conflict of interest

The authors declare no conflicts of interest.

Data availability statement

Data supporting these findings are available within the article or upon request.

Institutional review board statement

Not applicable.

Informed consent statement

Not applicable.

Additional information

Received: 2025-04-11

Accepted: 2025-06-23

Published: 2025-07-02

Academia Materials Science papers should be cited as *Academia Materials Science 2025*, ISSN 2997-2027, https://doi.org/10.20935/AcadMatSci7795. The journal's official abbreviation is *Acad. Mat. Sci.*

Publisher's note

Copyright

References

1. Jose SA, John M, Menezes PL. Cermet systems: synthesis, properties, and applications. Ceramics. 2022;5(2):210–36. doi: 10.3390/ceramics5020018

2. Strondl A, Lyckfeldt O, Brodin H, Ackelid U. Characterization and control of powder properties for additive manufacturing. JOM. 2015;67:549–54. doi: 10.1007/s11837-015-1304-0

3. Ziegelmeier S, Christou P, Wöllecke F, Tuck C, Goodridge R, Hague R, et al. An experimental study into the effects of bulk and flow behavior of laser sintering polymer powders on resulting part properties. J Mater Process Technol. 2015;215:239–50. doi: 10.1016/j.jmatprotec.2014.07.029

4. Miranda F, dos Santos MO, Condotta R, Pereira NMG, Rodrigues D, Janasi SR, et al. Additive manufacturing of tungsten carbide (WC)-based cemented carbides and niobium carbide (NbC)-based cermets with high binder content via laser powder bed fusion. Metals. 2024;14(12):1333. doi: 10.3390/met14121333

5. Balc N, Berce P, Pacurar R. Comparison between SLM and SLS in producing complex metal parts. Proceedings of the Annals of DAAAM and Proceedings of the International DAAAM Symposium; 2010 Oct 20–23; Zadar, Croatia; 2010 [cited 2025 Jan 27]. Available from: https://www.daaam.info/Downloads/Pdfs/proceedings/proceedings_2010/17059_Annals_4_head.pdf

6. Riener K, Albrecht N, Ziegelmeier S, Ramakrishnan R, Haferkamp L, Spierings AB, et al. Influence of particle size distribution and morphology on the properties of the powder feedstock as well as of AlSi10Mg parts produced by laser powder bed fusion (LPBF). Add Manufact. 2020;34:101286. doi: 10.1016/j.addma.2020.101286

7. Sidambe AT, Tian Y, Prangnell P, Fox P. Effect of processing parameters on the densification, microstructure, and crystallographic texture during the laser powder bed fusion of pure tungsten Intern J Refractory Metals Hard Mater. 2019;78:254–63. doi: 10.1016/j.ijrmhm.2018.10.004

8. Xing M, Wang H, Zhao Z, Lu H, Liu C, Lin L, et al. Additive manufacturing of cemented carbides inserts with high mechanical performance. Mater Sci Eng A. 2022;861:144350. doi: 10.1016/j.msea.2022.144350

9. Lüddecke A, Pannitz O, Zetzener H, Sehrt JT, Kwade A. Powder properties and flowability measurements of tailored nanocomposites for powder bed fusion applications. Mater Des. 2021;202:109536. doi: 10.1016/j.matdes.2021.109536

10. Mehrabi M, Gardy J, Talebi FA, Farshchi A, Hassanpour A, Bayly AE. An investigation of the effect of powder flowability on the powder spreading in additive manu-facturing. Powder Technol. 2023;413:117997. doi: 10.1016/j.powtec.2022.117997

11. Marchetti L, Hulme-Smith C. Flowability of steel and tool steel powders: A comparison between testing methods. Powder Technol. 2021;384:402–13. doi: 10.1016/j.powtec.2021.01.074

12. Santos LC, Condotta R, Ferreira MC. Flow properties of coarse and fine sugar powders. J Food Proc Eng. 2018;41(2):12648. doi: 10.1111/jfpe.12648

13. Spierings AB, Herres N, Levy G. Influence of the particle size distribution on surface quality and mechanical properties in AM steel parts. Rapid Prototyp J. 2011;17(3):195–202. doi: 10.1108/13552541111124770

14. Miranda F, dos Santos MO, Rodrigues D, Coelho RS, Batalha GF. NbC-based cermet production comparison: L-PBF additive manufacturing versus conventional LPS powder metallurgy. Mater Technol. 2023;57(5):465–73. doi: 10.17222/mit.2023.972

15. Fernandes LJ, Stoeterau RL, Batalha GF, Rodrigues D, Borrile AV. Wear analysis of NbC-Ni cemented carbides for cutting tools. Adv Mater Process Technol. 2020;8(1):305–21. doi: 10.1080/2374068X.2020.1808925

16. Mannesson K. WC grain growth during sintering of cemented carbides-Experiments and simulations [Doctoral Thesis]. Stockholm: Universitet Service US AB; 2011 [cited 2024 Sep 14]. Available from: http://www.diva-portal.org/smash/get /diva2:410627/FULLTEXT01.pdf

17. Labonne M, Missiaen J-M, Lay S, García N, Lavigne O, García LF, et al. Sintering behavior and microstructural evolution of NbC-Ni cemented carbides with Mo2C additions. Int J Refract Met Hard Mater. 2020;92:105295. doi: 10.1016/j.ijrmhm.2020.105295

18. Huang SG, Li L, Van Der Biest O, Vleugels J. Influence of WC addition on the microstructure and mechanical properties of NbC-Co cermets. J Alloys Compd. 2007;430(1–2):158–64. doi: 10.1016/j.jallcom.2006.05.015

19. Freeman R. Measuring the flow properties of consoli-dated, conditioned and aerated powders: a comparative study using a powder rheometer and a rotational shear cell. Powder Technol. 2007;174(1–2):25–33. doi: 10.1016/j.powtec.2006.10.016

20. Hare C, Zafar U, Ghadiri M, Freeman T, Clayton J, Murtagh M. Analysis of the dynamics of the FT4 powder rheometer. Powder Tech. 2015;285:123–7. doi: 10.1016/j.powtec.2015.04.039

21. Zegzulka J, Gelnar D, Jezerska L, Prokes R, Rozbroj J. Characterization and flowability methods for metal powders. Sci Rep. 2020;10:21004. doi: 10.1038/s41598-020-77974-3

22. Ortega-Rivas E. Unit operations of particulate solids: theory and practice. Abingdon: Taylor and Francis; 2012.

23. Rhodes M. Introduction to particle technology. Hoboken (NJ): Wiley; 2008.

24. Budding A, Vaneker T. New strategies for powder compaction in powder-based rapid prototyping techniques. Procedia CIRP. 2013;6:528–33. doi: 10.1016/j.procir.2013.03.100

25. Huang JH, Huang SG, Zhou P, Lauwers B, Qian J, Vleugels J. Microstructure and mechanical properties of WC or Mo2C modified NbC-Ni cermets. Int J Refract Met Hard Mater. 2021;95:105440. doi: 10.1016/j.ijrmhm.2020.105440

26. Li J, Wei Z, Zhou B, Wu Y, Chen S-G, Sun Z. Densification, microstructure and properties of 90W-7Ni-3Fe fabricated by selective laser melting. Metals. 2019;9:884. doi: 10.3390/met9080884

27. Campanelli S, Contuzzi N, Posa P, Angelastro A. Printability and microstructure of selective laser melting of WC/Co/Cr powder. Materials. 2019;12:2397. doi: 10.3390/ma12152397

28. Wang D., Yu C., Zhou X., Ma J., Liu W., Shen Z. Dense pure tungsten fabricated by selective laser melting. Appl Sci. 2017;7:430. doi: 10.3390/app7040430

29. Pötschke J. Additive Manufacturing of hard metals: an evaluation of potential processes for tool production. Met Addit Manuf. 2020;6(3):155–62. [cited 2024 Nov 6]. Available from: https://www.metal-am.com/wp-content/uploads/sites/4/2020/10/Metal-AM-Autumn-2020.pdf

30. Huang SG, Liu BL, Liu C, Vleugels J, Huang JH, Answer Z, et al. Tailoring microstructure and mechanical properties of NbC-Ni matrix cermets for wear resistance applications. Proceedings of the 20th Plansee Seminar on Refractory Metals and Hard Materials; 2022 May 30–Jun 3; Reutte, Austria; 2022.